Earth and Planetary Science Letters 463 (2017) 221–231

Contents lists available at ScienceDirect

Earth and Planetary Science Letters

www.elsevier.com/locate/epsl

Production of nanoparticles during experimental deformation of smectite and implications for seismic slip

S. Aretusini [a,*], S. Mittempergher [b], O. Plümper [c], E. Spagnuolo [d], A.F. Gualtieri [e], G. Di Toro [a,d,f]

[a] School of Earth and Environmental Sciences, University of Manchester, Manchester, UK
[b] Dipartimento di Scienze della Terra, Università degli Studi di Torino, Torino, Italy
[c] Department of Earth Sciences, Utrecht University, Utrecht, The Netherlands
[d] Sezione di Tettonofisica e Sismologia, Istituto Nazionale di Geofisica e Vulcanologia, Roma, Italy
[e] Dipartimento di Scienze Chimiche e Geologiche, Università degli Studi di Modena e Reggio Emilia, Modena, Italy
[f] Dipartimento di Geoscienze, Università degli Studi di Padova, Padova, Italy

A R T I C L E I N F O

Article history:
Received 15 September 2016
Received in revised form 30 January 2017
Accepted 31 January 2017
Editor: J. Brodholt

Keywords:
smectite
earthquakes
friction
nanoparticles
clay amorphization

A B S T R A C T

Nanoparticles and amorphous materials are common constituents of the shallow sections of active faults. Understanding the conditions at which nanoparticles are produced and their effects on friction can further improve our understanding of fault mechanics and earthquake energy budgets. Here we present the results of 59 rotary shear experiments conducted at room humidity conditions on gouge consisting of mixtures of smectite (Ca-montmorillonite) and quartz. Experiments with 60, 50, 25, 0 wt.% Ca-montmorillonite, were performed to investigate the influence of variable clay content on nanoparticle production and their influence on frictional processes. All experiments were performed at a normal stress of 5 MPa, slip rate of $0.0003 \leq V \leq 1.5$ ms^{-1}, and at a displacement of 3 m. To monitor the development of fabric and the mineralogical changes during the experiments, we investigated the deformed gouges using scanning and transmission electron microscopy combined with X-ray powder diffraction quantitative phase analysis. This integrated analytical approach reveals that, at all slip rates and compositions, the nanoparticles (grain size of 10–50 nm) are partly amorphous and result from cataclasis, wear and mechanical solid-state amorphization of smectite. The maximum production of amorphous nanoparticle occurs in the intermediate slip rate range ($0.0003 \leq V \leq 0.1$ ms^{-1}), at the highest frictional work, and is associated to diffuse deformation and slip strengthening behavior. Instead, the lowest production of amorphous nanoparticles occurs at co-seismic slip rates ($V \geq 1.3$ ms^{-1}), at the highest frictional power and is associated with strain and heat localization and slip weakening behavior. Our findings suggest that, independently of the amount of smectite nanoparticles, they produce fault weakening only when typical co-seismic slip rates (>0.1 ms^{-1}) are achieved. This implies that estimates of the fracture surface energy dissipated during earthquakes in natural faults might be extremely difficult to constrain.

© 2017 Elsevier B.V. All rights reserved.

1. Introduction

Amorphous and crystalline nanoparticles are common constituents of the shallow sections of natural faults (Chester et al., 2005; Ma et al., 2006). As a consequence, a general issue in fault mechanics is how nanoparticles form and what role they have in the seismic cycle (Sammis and Ben-Zion, 2008). For instance, the presence of nanoparticles can favor the activation of grain size-dependent deformation processes (De Paola et al., 2015) and enhance the reaction kinetics at both seismic and sub-seismic slip rates (Hirono et al., 2013). Moreover, the reduction in grain size of fault materials during seismic rupture propagation and slip affects the earthquake energy budget (Chester et al., 2005; Ma et al., 2006; Reches and Dewers, 2005). Production of nanoparticles increases some energy sinks (e.g., the breakdown work or the energy dissipated during rupture propagation, Tinti et al., 2005) at the expense, for instance, of the seismic radiated energy (Kanamori and Rivera, 2006). Here, given the abundance of smectite-rich gouges in natural faults, we focus on the investigation of the deformation

* Corresponding author at: School of Earth and Environmental Sciences, The University of Manchester, Williamson Building, Oxford Road, Manchester M13 9PL, UK.
E-mail address: stefano.aretusini@postgrad.manchester.ac.uk (S. Aretusini).

http://dx.doi.org/10.1016/j.epsl.2017.01.048
0012-821X/© 2017 Elsevier B.V. All rights reserved.

conditions that lead to the production of nanoparticles in these materials.

Smectite minerals, i.e. hydrous aluminum phyllosilicates, are common gouge constituents in shallow fault zones, and are among the major components of fault cores sampled during the scientific drilling of several seismogenic faults (e.g., Chester et al., 2013; Holdsworth et al., 2011; Kuo et al., 2009; Ohtani et al., 2000; Schleicher et al., 2010). Detailed microstructural studies on gouge samples from scientific drilling in the Nojima fault (Janssen et al., 2013), the San Andreas fault (Janssen et al., 2010), and the Chelungpu fault (Janssen et al., 2014; Kuo et al., 2009) reported amorphous and nanocrystalline materials associated with smectite-rich fault rocks. These materials included glass, amorphous rims around quartz grains, and partly to fully amorphous nanoparticles, often associated with recrystallized smectite minerals (Janssen et al., 2013; Kuo et al., 2009; Schleicher et al., 2010). Amorphous materials and nanoparticles have also been described in exhumed fault rocks, formed at the expense of granitic (Ozawa and Takizawa, 2007) and graphite-rich gouges (Nakamura et al., 2015). In general, understanding the processes and conditions that lead to nanoparticles and amorphous materials production in fault rocks, will help to interpret the chemical and physical processes active during the seismic cycle at shallow depths.

The production of nanoparticles can occur by cataclasis, wear, and mechanical solid state amorphization, which can reduce initial grain size down to less than 100 nm and introduce lattice defects in the crystalline solids (e.g., Hadizadeh et al., 2015; Yund et al., 1990). During and immediately after seismic slip the temperature increase in the slipping zone due to frictional heating enhances diffusional processes and may facilitate recovery of lattice defects and decrease the degree of amorphization (De Castro and Mitchell, 2002).

The effect of nanoparticles on bulk friction has been explored mainly for granitoid and carbonatic rocks and gouges (De Paola et al., 2015; Green et al., 2015). The extremely small size and high specific surface area of nanoparticles may promote grain-size dependent deformation processes (i.e. superplastic behavior (Ashby and Verrall, 1973)), resulting in fault weakening at seismic slip rates (∼1 m/s) and rate-weakening behavior at sub-seismic slip rates (Verberne et al., 2014). However, the processes of nanoparticle production and its effect on bulk friction at seismic slip rates in clay-rich gouges have yet to be systematically studied (Remitti et al., 2015).

Here we quantify the production of nanoparticles in smectite-bearing gouges and their effect on friction by combining rotary shear experiments with a systematic mineralogical and microstructural characterization of the experimental products. Using this information, we discuss the processes leading to the production of nanoparticles and how they influence energy partitioning and dynamic weakening during seismic slip (0.0003–1.5 ms^{-1}). Our conclusions apply to seismic, clay-rich faults at shallow crustal depth.

2. Methods

2.1. Starting material

Since variable proportions of smectite and quartz occur in fault cores of plate boundary faults (e.g. Kameda et al., 2015), we used four different compositions to control the effect of smectite content on nanoparticles production. We tested four materials including (i) STx-1b source clay with 60 wt.% Ca-Montmorillonite (Ca-mnt), 20 wt.% opal-CT (opal) and 20 wt.% amorphous material, purchased from Clay Minerals Society (see Section 3.2 and Table 1 for their mineral composition) (Chipera and Bish, 2001), (ii) pure crystalline quartz powder, commercially known as "micronized quartz", (iii) 80:20 weight proportions of STx-1b and micronized quartz to obtain 50 wt.% Ca-mnt-rich gouges, and (iv) 40:60 weight proportions of STx-1b and micronized quartz to obtain 25 wt.% Ca-mnt-rich gouges. Before each experiment, the starting materials were equilibrated at room humidity conditions (20–45% relative humidity).

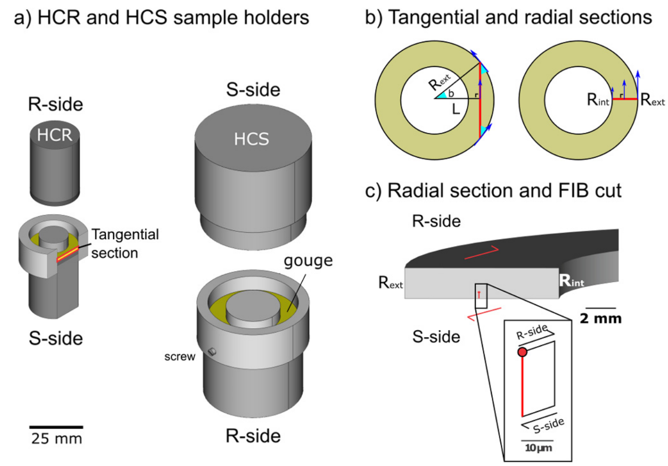

Fig. 1. a) The sample assemblage of the experiments performed with ROSA (HCR) and SHIVA (HCS) comprised two hollow stainless steel specimen holders (medium gray) with, respectively, 7.5/12.5 and 15/25 mm inner/outer radii (R_{int}/R_{ext}). To confine the gouge (yellow) two Teflon parts (light grey) were used: a cylinder inserted in the inner hole and a ring positioned externally. The outer ring was cut at ∼60° to its basal surface and tightened to the metal gouge holders with a stainless steel hose clamp. In the SHIVA experiments the Teflon components were fixed with screws to the specimen metal holder. The red cross-sections represent the tangential section on HCR. b) Tangential and radial sections geometry. The tangential section is cut at a distance from the axis $L = 0.5 \cdot (R_{int} + R_{ext})$. Because of this, from the center to the edge of the section, radius r varies as $R_{ext} \leq r \leq L$ and b, the angle between the section and the slip vector (blue arrows), varies as $0° \leq b \leq 37°$ (according to $b = \arccos(L/R_{ext})$). In the radial section geometry, radius r varies as $R_{int} \leq r \leq R_{ext}$ and angle b is always 90°. c) Orientation of the FIB cut. The FIB cut is orthogonal to the radial section, therefore is parallel to the slip vector, with shear sense as indicated. (For interpretation of the references to color in this figure legend, the reader is referred to the web version of this article.)

Scanning electron microscope (SEM) investigations conducted on 60 wt.% Ca-mnt revealed that the gouge had a granular appearance (grain size <100 μm, Supplementary Fig. 1). The individual grains consisted of micrometer-sized Ca-mnt with a fibrous-like appearance, encompassing opal grains (grain size <5 μm). Because of their intimate association, we could not separate Ca-mnt grains from opal grains. The micronized quartz powder was made of angular quartz grains (grain size <100 μm).

2.2. Rotary shear experiments

Rotary shear apparatuses are currently the only experimental equipment imposing deformation conditions at seismic slip rates ($0.0001 \leq V \leq 10$ ms^{-1}) for displacements (>0.3 m) typical of moderate to large earthquakes. To control the reproducibility of experiments we used two rotary shear apparatuses: ROSA (ROtary Shear Apparatus, model MIS-233-1-77 from MARUI & CO., LTD (Rempe et al., 2014)), installed at the University of Padova (Padua, Italy) and SHIVA (Slow to High Velocity Apparatus (Di Toro et al., 2010)), installed at the Istituto Nazionale di Geofisica e Vulcanologia (Rome, Italy). The sample assemblages for both rotary apparatuses are described in Fig. 1a.

The gouges were sheared for 3 m of equivalent displacement under a normal stress of 5 MPa (for definition of equivalent displacement, velocity, etc. see Di Toro et al., 2010). Hereafter, equivalent velocity and equivalent displacement will be referred to as slip rate and displacement, respectively. In ROSA, experiments with 60, 50 and 25 wt.% Ca-mnt were performed at slip rates of 0.0003, 0.001, 0.01, 0.1, 0.3, 1.3, 1.5 ms^{-1}, while experiments with pure quartz powders were performed at slip rates of 0.01, 0.1, 1.3 ms^{-1}.

Download English Version:

https://daneshyari.com/en/article/5780106

Download Persian Version:

https://daneshyari.com/article/5780106

Daneshyari.com